Title	Ultimate Load of Slabs in Fire Enhanced by Tensile Membrane Action with Flexible Supporting Edge Beams
Author(s)	Tan, Kang-Hai; Nguyen, Tuan-Trung
Citation	Tan, K.H., & Nguyen, T.-T. (2014). Ultimate Load of Slabs in Fire Enhanced by Tensile Membrane Action with Flexible Supporting Edge Beams. 8th International Conference on Structures in Fire.
Date	2014
URL	http://hdl.handle.net/10220/40801
Rights	© 2014 ETH Zurich. This is the author created version of a work that has been peer reviewed and accepted for publication by 8th International Conference on Structures in Fire, ETH Zurich. It incorporates referee's comments but changes resulting from the publishing process, such as copyediting, structural formatting, may not be reflected in this document. The published version is available at: [http://www.cnki.net/kcms/detail/detail.aspx?dbname=IPFDTEMP&filename=SHCB201406001036&dbcode=IPFD&v=MDAwNDE3cVFLcmlmWnVCdkVDdmpVN3ZJSVZvUU5pWEliTEc0SDlYTXFZOUZaZXNNQ2hNNHptVVdtVDhJVGdyZ3F4TkdE].

8th International Conference on Structures in Fire
Shanghai, China, June 11-13, 2014

ULTIMATE LOAD OF SLABS IN FIRE ENHANCED BY TENSILE MEMBRANE ACTION WITH FLEXIBLE SUPPORTING EDGE BEAMS

Kang-Hai Tan*, Tuan-Trung Nguyen*

* Nanyang Technological Univ., School of Civil and Environmental Engineering, Singapore
e-mails: CKHTAN@ntu.edu.sg, nguyentt@ntu.edu.sg

Keywords: Tensile membrane action, Beam-slab systems, Slabs, Flexible support, Fire, Analytical

Abstract. *A number of previous analytical studies have been conducted to predict the enhanced load-bearing capacity of slabs due to tensile membrane action. These analytical approaches are based on an implicit assumption that vertical supports along the slab panel boundaries at all times during a fire do not deform. In reality the edge beams do deform even though they are fire-protected, and thus this assumption may be nullified. This renders their predictions to be unconservative when there is significant deflection of protected edge beams. This work looks at the actual condition where the protected supporting edge beams do deflect, and the slab still bends in synclastic curvature. The authors propose a semi-analytical model which can predict the load-bearing capacity of the composite beam-slab floor systems under fire conditions enhanced by tensile membrane action, but reduced by deflection of the protected edge beams. Its feature is that the deflection of the protected edge beams can be taken into account of calculation of the slab enhancement factor.*

1 INTRODUCTION

At ambient temperature, the applied load on the slab in a composite floor system is distributed from the slab to the secondary beams in one-way action. The load path involved in resisting the permanent and variable loads under ambient condition is: slab → secondary beams → main beams → columns.

Under severe fire conditions, if the secondary interior beams are unprotected, due to degradation of strength in fire they lose most of their strength. As a result, the beams form plastic hinges and the load path at ambient temperature cannot be maintained. The load-carrying mechanism changes to a two-way bending system. The region involving the slab and the unprotected interior beams is known as *a slab panel*. Under severe fire conditions, the load applied to a slab panel is distributed in a load path as follows: slab → supporting edge beams → columns.

The slab panel develops its load-bearing capacity in the deformed state through a combination of yield-line mechanism and tensile membrane action. A number of analytical studies [1-4] have attempted to predict the enhanced load-bearing capacity of slab due to TMA. Among these approaches, a well-known approach, namely, the Bailey-BRE method [1], has been adopted in the SCI Publication P288 [5] and applied in the UK practice. These analytical approaches are based on an implicit assumption that vertical supports along the slab panel boundaries at all times during a fire do not deform. The task of providing the necessary vertical support requires the edge beams to be sufficiently protected so that deflections are small. This is so that the slab can bend in synclastic curvature.

However, in reality the edge beams do deform even though they are fire-protected, and thus this assumption may be nullified. This renders their predictions to be unconservative when there is significant deflection of protected edge beams. On the other hand, tensile membrane action can still be mobilised although the protected edge beams deform, provided that the plastic hinges do not form on the edge beams. Once the plastic hinges form on the protected edge beams, tensile membrane action will disappear.

The authors' work presented in this paper looks at the actual condition where the protected supporting edge beams do deflect, and the slab still bends in synclastic curvature. The authors propose a semi-analytical model to predict the load-bearing capacity of the slab enhanced by tensile membrane action, but reduced by deflection of the protected edge beams. The proposed model was developed based on the BRE-Bailey method. The innovative feature is that the proposed model can take account of vertical deflection of the protected edge beams.

2 PROPOSED SEMI-ANALYTICAL METHOD

2.1 Assumptions

The following assumptions are adopted in the model: (1) the slab panel is assumed to be unrestrained against horizontal movement, and supported along four edges by the protected beams; (2) the load supported by the flexural behaviour of the composite slab is calculated based on the lower-bound yield-line mechanism, assuming that the interior beams have zero resistance; (3) the protected edge beams are assumed to be simply supported without any lateral restraint; (4) the load distribution on the edge beams at collapse follows the shape of the segments of the yield line mechanism, i.e. triangular loading distribution for the short-span beams and trapezoidal loading distribution for the long-span beams; (5) torsional rigidity of the edge beams is assumed to be negligible; (6) the load-carrying capacity of *the steel interior beams* and the slab (enhanced due to membrane action) are added together.

Based on the author's test results [6], the second assumption is accurate and conservative. Therefore, the slab panel is considered unrestrained against horizontal movement in the proposed model.

When calculating the load capacity of the slab, the proposed model uses the second assumption, in which the lower-bound yield-line mechanism in the slab is adopted. This is a short coming of the proposed model since it cannot take into account the interaction between the slab and the unprotected interior beams. The contribution of the unprotected interior beams on the load capacity of the composite beam-slab system in fire is considered by the sixth assumption.

In the sixth assumption, when calculating the additional load supported by unprotected interior beams in fire, the beams should be considered as steel beams. To validate this assumption, comparisons between the proposed model and the test results are conducted with two cases, i.e. the interior beams are treated as composite beams and as steel beams. They are not presented in this paper.

2.2 Failure modes

A composite floor system may fail due to failure mechanism of the slab panel or due to the composite beam-slab collapse mechanisms which involve failure of both the panel and the beams. These two failure mechanisms, *i.e. single slab panel* (Figure 1) *and beam-slab collapse mechanisms* (Figure 2), are the two failure mode mechanisms.

In terms of the failure mode of the slab panel alone, Bailey and Toh [7] proposed two failure modes as shown in Figure 1, based on their fire tests conducted on isolated slabs. The first failure mode is due to fracture of the mesh reinforcement across the short span at the centre of the slab. A second failure mode occurs due to crushing of the concrete in the corners of the slab where high compressive in-plane forces develop.

As observed in the authors' tests [6], the authors adopt these two failure modes of the slab panel (Figure 1) in estimating the enhancement factor of the slab due to TMA.

The composite beam-slab collapse mechanisms may appear if plastic hinges form in the perimeter beams and the yield lines occur across the centre of the slab as shown in Figure 2. These collapse mechanisms were proposed by Abu *et al.* [8] and have been included in SCI Publication P390 [9].

The most important condition for the mobilisation of TMA is that the slab must bend in synclastic curvature. Once the 'folding' mechanism has formed, TMA will vanish, leading to failure of the system. Therefore, the edge beams must be checked to ensure a minimum required moment resistance in order that the composite collapse mechanisms do not occur. Verification of the resistance of the edge beams [9]

must be conducted in order to ensure that the failure mechanisms of single slab panel (Figure 1) will occur.

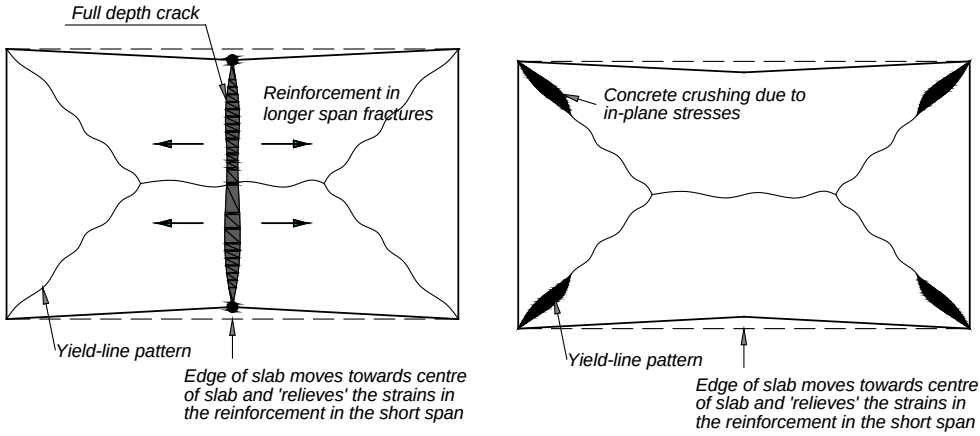

a) Tensile failure of mesh reinforcement b) Compressive failure of concrete

Figure 1. Assumed failure modes for isolated slab panels [7]

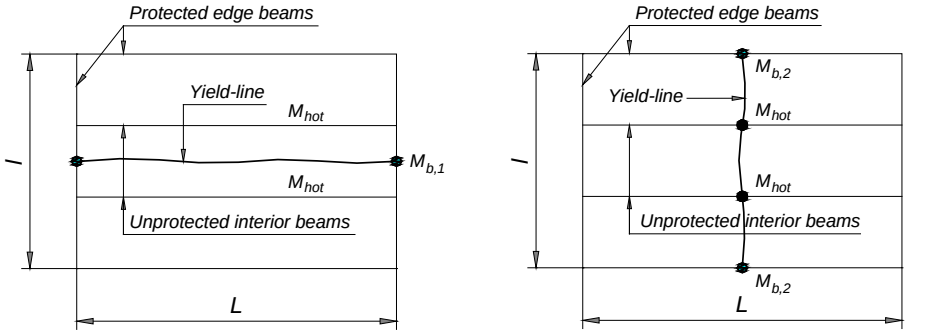

a) Yield line parallel to the unprotected beam b) Yield line perpendicular to the unprotected beam

Figure 2. Composite collapse mechanisms [8]

2.3 Proposed enhancement factor

The authors propose a semi-analytical model which can predict the load-bearing capacity of the slab enhanced by tensile membrane action by taking account of vertical deflections of the protected edge beams. The proposed model was developed based on the BRE-Bailey method [7], in which the load supported by the flexural behaviour of the composite slab is calculated based on the lower-bound yield-line mechanism, assuming that the interior beams have zero resistance. The overall enhancement factor can be calculated by Eq. (1). The deformed shape of a slab-beam floor system is shown in Figure 3.

$$\begin{aligned} e_1^* &= e_{1m}^* + e_{1b} \\ e_2^* &= e_{2m}^* + e_{2b} \end{aligned} \tag{1}$$

and the overall enhancement is given by:

$$e^* = e_1^* - \frac{e_1^* - e_2^*}{1 + 2\mu a^2} \tag{2}$$

where e_{1m}^* and e_{2m}^* are the contribution of membrane forces to load bearing capacity of elements 1 and 2, respectively; e_{1b} and e_{2b} are the factors which take into account of the effect of membrane forces on the bending resistance due to the presence of axial force of elements 1 and 2, respectively.

The predicted load bearing capacity of the slab enhanced by TMA is calculated by Eq. (3):

$$q_{s,\theta} = e^* \times p_{y,\theta} \tag{3}$$

where $p_{y,\theta}$ is the yield-load of the slab at temperature θ.

In the Bailey-BRE method, the values e_1 and e_2 are calculated based on the equilibrium of elements 1 and 2 with *the vertical rigid supports*. Therefore, the method has to assume that the supports along the edges of the slab panel remain rigid, and it cannot consider vertical deflections of the edge beams.

In the proposed approach, the values e_1^* and e_2^* are calculated based on the equilibrium of elements 1 and 2 with *the vertical deformed supports*. Deflection of the edge beams is determined based on the deflected shape.

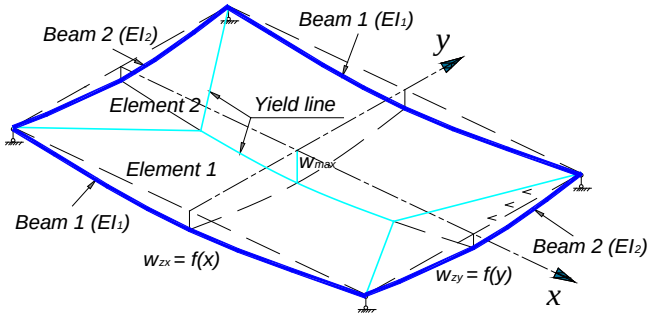

Figure 3. Deformed shape of a slab-beam floor system

2.4 In-plane stress distribution

The inplane stress distribution is assumed to be similar to the Bailey-BRE method as shown in Figure 4. It is assumed that the in-plane forces comprise compressive membrane forces around the perimeter of the slab and tensile membrane forces in the central area of the slab. The magnitude of the forces is defined by the constants *k* and *b* which depend on the dimensions of the slab. The derivations of the inplane stress distribution are conducted by Hayes [10] and Bailey and Moore [1]. Only the results are given below.

The parameters *k* and *b* are determined from equilibrium of the in-plane stress distribution. The intersection point of the yield lines is defined by the parameter *n* calculated using the yield-line theory.

$$k = \frac{4na^2(1-2n)}{4n^2a^2+1} + 1 \quad ; \quad n = \frac{1}{2\sqrt{\mu a^2}}\left[\sqrt{3\mu a^2 + 1} - 1\right] \le 0.5 \tag{4}$$

where a is the aspect ratio of the slab (L/l) and μ is the ratio of the yield moment capacity of the slab in orthogonal directions (should always be less than or equal to 1.0).

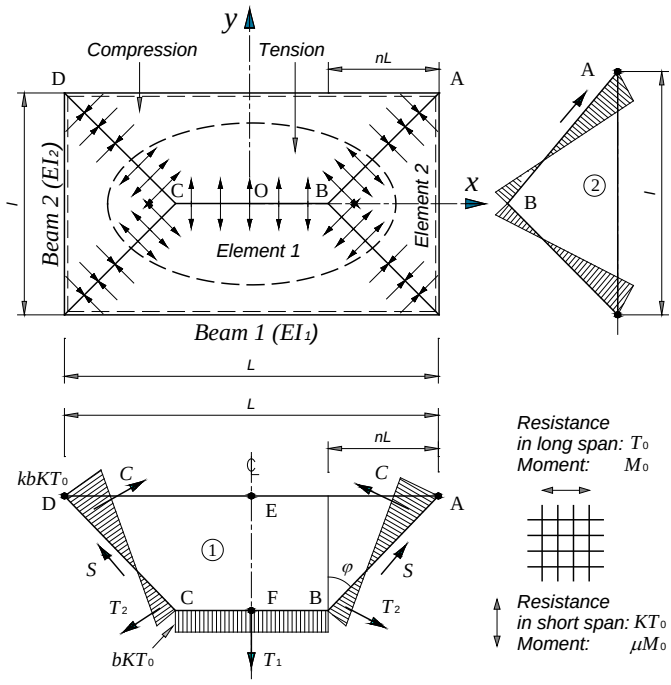

Figure 4. In-plane stress distribution for membrane action

The yield-line resistance of the slab panel at temperature θ can be calculated by Eq. (5).

$$p_y = \frac{24\mu M_0}{l^2}\left[\sqrt{3+\frac{1}{\left(\sqrt{\mu}a\right)^2}}-\frac{1}{\sqrt{\mu}a}\right]^{-2} \tag{5}$$

The constant b is chosen as the minimum value in the following two expressions, which are associated with two failure modes of the slab as shown in Figure 1(a) and (b):

$$b=\frac{1.1l^2}{8K(A+B+C-D)} \quad ; \quad b=\frac{1}{kKT_0}\left[0.85 f_{ck}\,0.45\left(\frac{d_1+d_2}{2}\right)-T_0\left(\frac{K+1}{2}\right)\right] \tag{6}$$

where d_1 and d_2 are the effective depths in both orthogonal directions; A, B, C, D are the geometric parameters [7].

T_0 and KT_0 are the resistance of the reinforcing mesh per unit width in long and short spans, respectively. The bending moments M_0 and μM_0 per unit width of the slab in long and short spans respectively can be calculated by:

$$\mu M_0 = KT_0 d_1\left(\frac{3+(g_0)_1}{4}\right) \quad ; \quad M_0 = T_0 d_2\left(\frac{3+(g_0)_2}{4}\right) \tag{7}$$

where $(g_0)_1$ and $(g_0)_2$ are parameters which define the flexural stress block in short and long spans, respectively;

For element 1, the membrane force along the yield line BC (Figure 4) is constant and is equal to:

$$N_x\big|_{BC} = -bKT_0 \tag{8}$$

The membrane force along the yield line AB (element 1), at a distance of x from the centre point of the slab O is given by:

$$N_x\big|_{AB} = -bKT_0 + \frac{x-(L/2-nL)}{nL}(k+1)bKT_0 \tag{9}$$

The membrane force along the yield line for element 2, at a distance y from B can be expressed as:

$$N_y = -bKT_0 + \frac{y}{l/2}(k+1)bKT_0 \tag{10}$$

2.5 Out-plane stress distribution

Based on the fourth assumption, beam 1 (long-span beam) is subjected to a trapezoidal load with the maximum value $q_1 = ql/2$. Beam 2 (short-span beam) is subjected to a triangular load with the maximum value $q_2 = q(nL)$. The deformed shapes of beam 1 and beam 2 are $w_{zx}(x)$ and $w_{zy}(y)$, respectively. The deflection of the slab is w_m. The out-of-plane stress distribution is shown in Figure 5.

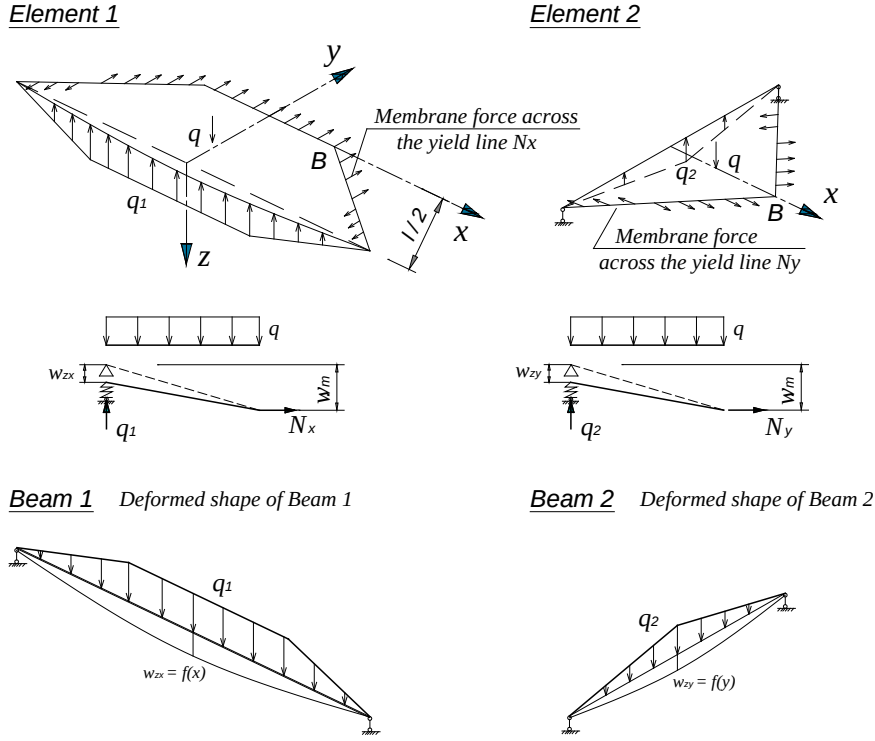

Figure 5. Out-of-plane stress distribution for membrane action

Deformed shape of the edge beams

Deflection of the edge beams (beams 1 and 2) at elevated temperatures consists of two components:

one from the trapezoidal load (beam 1) or from the triangular load (beam 2) transferred from the slab (Figures 6 & 7), and another from thermal gradient over the composite section of the edge beams.

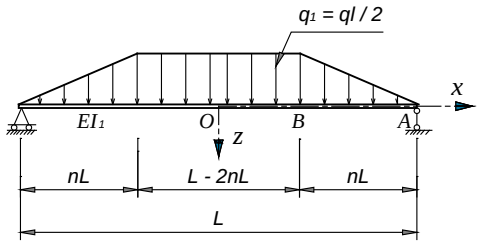

Figure 6. Load transferred to Beam 1

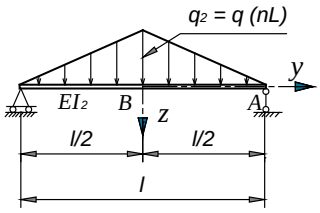

Figure 7. Load transferred to Beam 2

The deformed shape of beam 1 can be calculated by Eqs. (11) and (12).

Segment OB: $0 \le x \le L/2 - nL$:

$$w_{zx}^{(1)} = w_{zx\max} - \frac{1}{EI_1}\left[M_{xO} \times \frac{x^2}{2} - q_1 \frac{x^4}{24}\right] + \alpha T_{,zb1}\left(\frac{L^2}{8} - \frac{x^2}{2}\right) \tag{11}$$

Segment BA: $L/2 - nL \le x \le L/2$:

$$w_{zx}^{(2)} = w_{zx\max} - \frac{1}{EI_1}\left[M_{xO} \times \frac{x^2}{2} - q_1 \frac{x^4}{24}\right] - \frac{1}{EI_1}\frac{q_1}{nL}\frac{\left(x - (L/2 - nL)\right)^5}{120} + \alpha T_{,zb1}\left(\frac{L^2}{8} - \frac{x^2}{2}\right) \tag{12}$$

where $T_{,zb1}$ is the thermal gradient over the total depth of beam 1, α is the thermal expansion.

The maximum deflection $w_{zx\max}$ due to the load can be found from the boundary condition: $w_{zx}^{[2]} = 0$ at $x = L/2$.

$$w_{zx\max} = \frac{q_1}{EI_1}\left[\frac{1}{24}\left[8(nL)^2 + 12(nL)(L-2nL) + 3(L-2nL)^2\right] \times \frac{1}{8}L^2 - \frac{1}{24}\left(\frac{L}{2}\right)^4 + \frac{(nL)^4}{120}\right] \tag{13}$$

The maximum bending moment of the beam due to the load M_{xO} is:

$$M_{xO} = \frac{q_1}{24}\left[8(nL)^2 + 12(nL)(L-2nL) + 3(L-2nL)^2\right] \tag{14}$$

Substituting Eqs. (13) & (14) to (11) & (12), one can obtain the deformed shape of beam 1.

Similarly, the deflection Eq. for beam 2 due to both the load and the elevated temperatures is given in Eq. (15) with $0 \le y \le l/2$.

$$w_{zy}(y) = w_{zy\max} - \frac{1}{EI_2}\left[M_{yB} \times \frac{y^2}{2} - q_2 \frac{y^4}{24} + \frac{2}{l} q_2 \times \frac{y^5}{120}\right] + \alpha T_{,zb2}\left(\frac{l^2}{8} - \frac{y^2}{2}\right) \tag{15}$$

where $w_{zy\max}$ is the maximum deflection due to the load, and M_{yB} is the maximum bending moment of the beam due to the load:

$$w_{zy\max} = \frac{1}{120}\frac{q_2 l^4}{EI_2} \quad \text{and} \quad M_{yB} = \frac{1}{12} q_2 l^2 \tag{16}$$

Substituting Eq. (16) to (15), one can obtain the deformed shape of beam 2.

Contribution of membrane forces to load bearing capacity (e_{1m}^*, e_{2m}^*)

Taking moment about the support for element 1 (Figure 5), we have:

$$\int_{BC} N_x \left(w_m - w_{zx}^{(1)}\right) dx + 2\int_{AB} N_x \left(\frac{L/2-x}{nL} w_m - w_{zx}^{(2)}\right) dx - \text{Moment due to } \sum q = 0 \tag{17}$$

Substituting Eqs. (8), (9), (11) and (12) to (17):

$$\begin{aligned} &2\int_0^{L/2-nL} bKT_0 \left(w_m - w_{zx}^{(1)}\right) dx + 2\int_{L/2-nL}^{L/2} \left[bKT_0 - \frac{x-(L/2-nL)}{nL}(k+1)bKT_0\right] \times \left[\frac{L/2-x}{nL} w_m - w_{zx}^{(2)}\right] dx \\ &-q(L-2nL)\frac{l}{2}\frac{l}{4} - q \times nL \times \frac{l}{2} \times \frac{l}{6} = 0 \end{aligned} \tag{18}$$

It should be noted that $q_1 = ql/2$. After integrating and regrouping, with a slab deflection w_m, one can find a value of q according to Element 1 denoted as q_{1m}^* . The contribution of membrane forces to load bearing capacity according to Element 1 is given by:

$$e_{1m}^* = q_{1m}^* / p_{y,\theta} \tag{19}$$

where $p_{y,\theta}$ is the yield-line load of the slab at temperature θ.

Taking moment about the support for element 2 (Figure 5), we have:

$$2\int_{AB} N_y \left(\left(1 - \frac{y}{l/2}\right) w_m - w_{zy}\right) dy - \text{Moment due to } \sum q = 0 \tag{20}$$

Substituting Eqs. (10) and (15) to (20):

$$2\int_0^{l/2} \left[bKT_0 - \frac{y}{l/2}(k+1)bKT_0\right] \times \left[\left(1 - \frac{y}{l/2}\right) w_m - w_{zy}\right] dy - \frac{1}{6} ql \times (nL)^2 = 0 \tag{21}$$

It should be noted that $q_2 = q(nL)$. After integrating and regrouping, with a slab deflection w_m, one can find a value of q according to Element 2 denoted as q_{2m}^* . The contribution of membrane forces to load bearing capacity according to Element 2 is given by:

$$e_{2m}^* = q_{2m}^* / p_{y,\theta} \tag{22}$$

Effect of membrane forces on bending resistance capacity (e_{1b}, e_{2b})

The effect of the membrane forces on the bending resistance along the yield lines is evaluated by considering the yield condition when axial load is present. This effect does not depend on deflection of the edge beams. Therefore, the factors e_{1b} and e_{2b} are similar to the Bailey-BRE method [7].

After finding the factors e_{1m}^* and e_{2m}^* , the overall enhancement factor can be estimated by Eq. (2), and the load-bearing capacity of the slab enhanced by tensile membrane action can be found by Eq. (3).

3 MODEL VALIDATION

Verification of the resistance of the edge beams [9] must be conducted first in order to ensure that the failure mechanisms of single slab panel (Figure 1) will occur.

For each specimen, the test result was compared with the prediction from the Bailey-BRE method and the proposed model. For the specimens without unprotected interior beams, the comparisons were quite straightforward. For the specimens with unprotected interior beams, the bending resistance of

interior beams was calculated in order to check if these beams have failed. If the interior beams had failed, the total test load of 15.8 kN/m^2 was totally resisted by the slab. The enhancement factor determined from the test was compared with those calculated from the two models, i.e. the Bailey-BRE and the proposed approaches.

Since the Bailey-BRE method cannot consider deflection of the edge beams, the enhancement factor predicted by the Bailey-BRE method is calculated with the two deflections as shown in Eqs. (23) & (24).

$$\text{Absolute slab deflection: } w_m \tag{23}$$

$$\text{Relative slab deflection: } w_r = w_m - \frac{1}{2}\left(w_{MB} + w_{PSB}\right) \tag{24}$$

3.1 Specimens without unprotected interior beams

Among the authors' test series there were two specimens without interior beams, i.e. S1 and S3-FR. At the loading phase, the two specimens were loaded to a value of 15.8 kN/m^2, corresponding to a load ratio of about 2.0 for S1 and S3-FR, respectively. The tests were terminated when reinforcement fractured above the edge beams (S1) or compression ring crushed near the corners of the slab (S3-FR). More details of these specimens can be found in [6].

Table 1 Comparison of the proposed model and the Bailey-BRE model for the specimens without interior beams

Test	p_{test}	MB defl.	PSB defl.	Slab defl.	Total capacity			Prediction / Test		
					Bailey (Eq. 23)	Bailey (Eq. 24)	Model	Bailey (Eq. 23)	Bailey (Eq. 24)	Model
	kN/m^2	mm	mm	mm	kN/m^2	kN/m^2	kN/m^2			
S1	15.6	28	58	131	15.8	12.91	13.5	1.01	0.83	0.86
S3-FR	16.0	33	28	115	17.1	14.6	14.7	1.07	0.91	0.92
							M =	1.04	0.87	0.89

The comparisons for the specimens without unprotected interior beams are shown in Table 1. It can be seen that based on the absolute slab deflection (Eq. (23)), the Bailey-BRE method over-predicts the test results by 4%, whereas the method is conservative if the relative slab deflection is used instead (Eq. (24)). The proposed method predicts the test results more accurately than the Bailey-BRE method. It is because the authors' model can take into account the deflected shape of the edge beams. The discrepancy between the proposed model and the test results for these specimens is 11%.

3.2 Specimens with unprotected interior beams

Among the authors' test series there were six specimens with interior beams. Two specimens presented in the authors' companion paper, i.e. P215-M1099 and P486-M1099, are used here for the comparison.

Table 2 Comparison of the proposed model and the Bailey-BRE model for the specimens with interior beams

Test	p_{test}	MB defl.	PSB defl.	Slab defl.	Total capacity			Prediction / Test		
					Bailey (Eq. 23)	Bailey (Eq. 24)	Model	Bailey (Eq. 23)	Bailey (Eq. 24)	Model
	kN/m^2	mm	mm	mm	kN/m^2	kN/m^2	kN/m^2			
P215-M1099	15.6	38	57	124	18.0	14.2	15.0	1.15	0.91	0.96
P486-M1099	15.5	55	94	139	18.7	12.9	15.7	1.20	0.83	1.01
							M =	1.175	0.87	0.985

The comparisons for the specimens with unprotected interior beams are shown in Table 2. It can be seen that based on the absolute slab deflection, i.e. the deflection of the edge beams is not taken into account, the enhancement factors predicted by the Bailey-BRE method are greater than the test results by 17.5%. If the relative deflection is used instead, the Bailey-BRE method is conservative. The proposed model predicts the load-bearing capacity of composite beam-slab systems very well. The discrepancy between the proposed model and the test results for these specimens is only 1.5%.

4 CONCLUSIONS

This paper presents a semi-analytical model which can predict the load-bearing capacity of composite beam-slab floor systems under fire conditions enhanced by tensile membrane action, but reduced by deflection of the protected edge beams.

The proposed model was validated with the authors' test results conducted in Nanyang Technological University. The validations showed that the proposed model give conservative and more accurate predictions compared to the Bailey-BRE method. The model can take account of the beam-slab interactions under fire conditions and gives guidance on the required stiffness of edge beams which the Bailey-BRE method does not provide.

ACKNOWLEDGMENT

The research presented in this paper was funded by Agency for Science, Technology and Research (A*Star Singapore) under Grant No. M4070013. The financial support of A*Star is gratefully acknowledged.

REFERENCES

[1] Bailey C.G. and Moore D.B., "Structural behaviour of steel frames with composite floorslabs subject to fire: Part 1: Theory", *Structural engineer London*, 78(Compendex), 19-27, 2000a.

[2] Usmani A.S. and Cameron N.J.K., "Limit capacity of laterally restrained reinforced concrete floor slabs in fire", *Cement and Concrete Composites*, 26(2), 127-140, 2004.

[3] Zhang N.-S. and Li G.-Q., "A new method to analyze the membrane action of composite floor slabs in fire condition", *Fire Technology*, 46(Compendex), 3-18, 2010.

[4] Burgess I.W., Xu D., and Shan-Shan H. "An Alternative Simplified Model of Tensile Membrane Action of Slabs in Fire", *Application of Structural Fire Engineering (ASFE)*. 19-20 April 2013 Prague, Czech Republic361-367, 2013.

[5] Newman G.M., Robinson J.T., and Bailey C.G., *Fire Safe Design: A new Approach to Multi-Story Steel-Framed Buildings*, in *SCI Publication P288* 2006, The Steel Construction Institute.

[6] Nguyen T.T. and Tan K.H. "Testing of Composite Slab-beam Systems at Elevated Temperatures", *7th International Conference on Structures in Fire (SiF)*. 6-8 June 2012 Zurich, Switzerland, Swiss Federal Institute of Technology Zurich, 247-256, 2012.

[7] Bailey C.G. and Toh W.S., "Behaviour of concrete floor slabs at ambient and elevated temperatures", *Fire Safety Journal*, 42(6-7), 425-436, 2007.

[8] Abu A., Ramanitrarivo V., and Burgess I. "Collapse mechanisms of composite slab panels in fire", *6th International Conference on Structures in Fire, SiF'10, June 2, 2010 - June 4, 2010*. East Lansing, MI, United states, DEStech Publications Inc., 382-389, 2010.

[9] Simms W.I. and Bake S., *TSLAB V3.0 User Guidance and Engineering Update*, in *SCI Publication P390* 2010, The Steel Construction Institute.

[10] Hayes B., "Allowing for membrane action in plastic analysis of rectangular reinforced concrete slabs", *Magazine of Concrete Research*, 20(65), 205-212, 1968a.